materials design

VASP, Machine Learning, and Multi-Scale Physics: Defining the State of the Art in Materials Modeling

Martijn Marsman, University of Vienna and VASP GmbH
Erich Wimmer, Materials Design, Inc.

16-18 August 2022

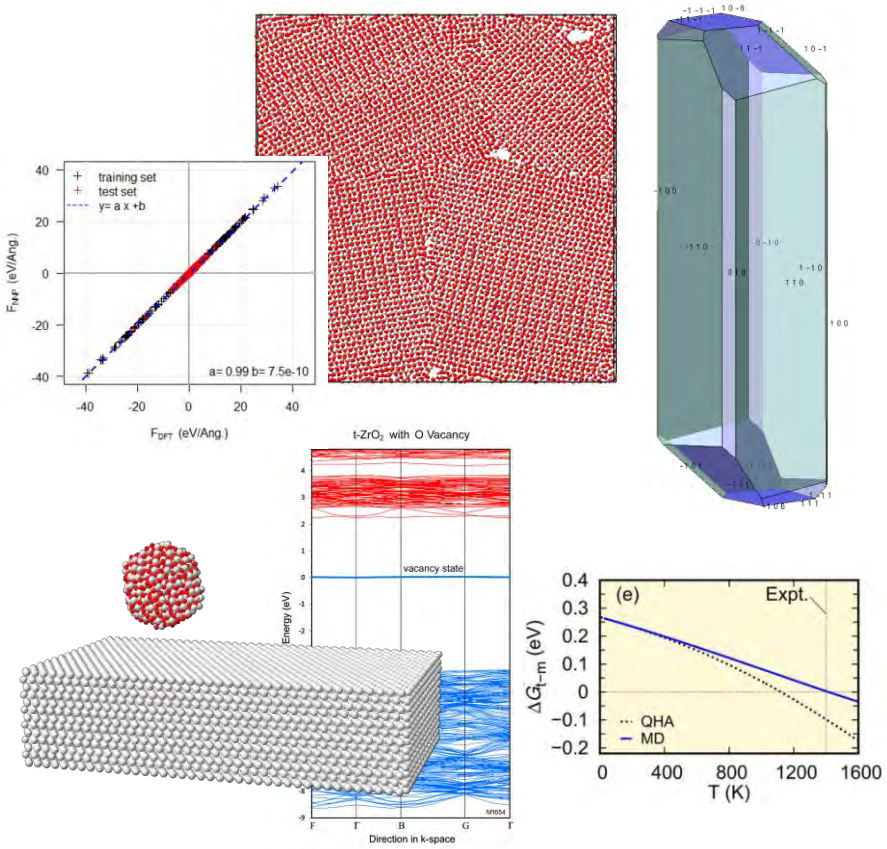

Materials Design Webinar Series

- Each session runs several times to accommodate schedules
  - Share the webinar series with your colleagues!
  - Registration details http://www.materialsdesign.com/webinars
- We will be recording this webinar
  - Watch any of our earlier webinars anytime
  - We will post upcoming webinars on the webinar page
- Vote for the next webinar topic!
  - Take a 2 minutes brief survey at the end of the webinar!
- Audio issues
  - Log out and log back in again
  - Check your audio output
  - Google Chrome (most recent 2 versions) Mozilla Firefox (most recent 2 versions) Apple Safari (most recent 2 versions) Microsoft Edge (most recent 2 versions)

materials design

Please Ask Questions!

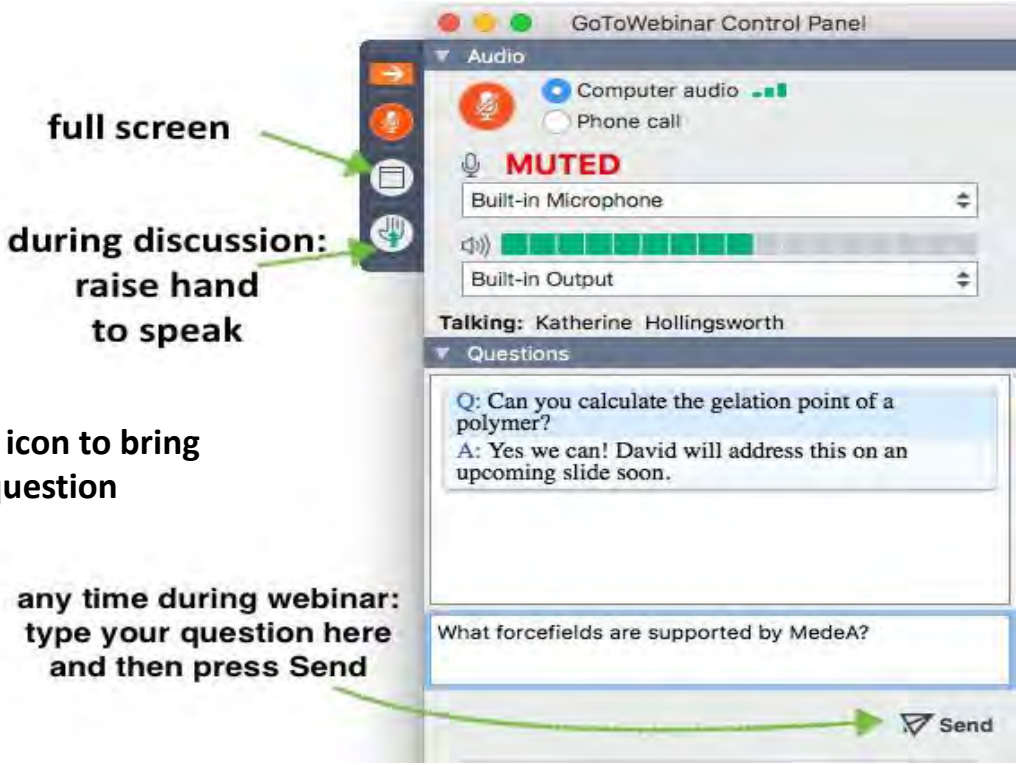

Use the raise hand icon to bring attention to your question

any time during webinar: type your question here and then press Send

materials design

Webinar Speakers

Katherine Hollingsworth

Martijn Marsman

Erich Wimmer

Erich Wimmer

Materials Design

Webinar Presenter

Martijn Marsman

University of Vienna

Webinar Presenter

materials design

VASP, Machine Learning, and Multi-Scale Physics: Defining the State of the Art in Materials Modeling

Martijn Marsman, University of Vienna and VASP GmbH
Erich Wimmer, Materials Design, Inc.

16-18 August 2022

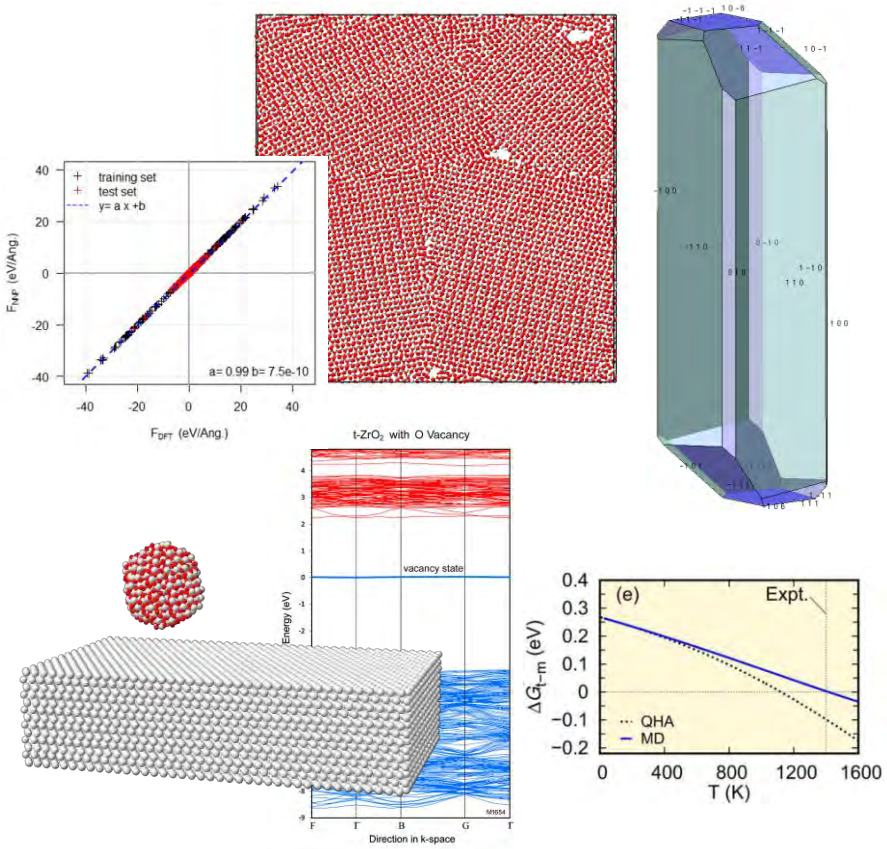

Agenda

- Machine Learning in Materials Research
- Multi-scale simulations
- VASP and machine-learned potentials - examples
  - Metals
  - Ceramics
- VASP and accuracy in large systems: delta learning
- Summary

Machine Learning in Materials Research

- Machine learning in data-driven approaches
- Machine-learned potentials for multi-scale simulations

- Both approaches rely on large, consistent, and accurate datasets that VASP delivers

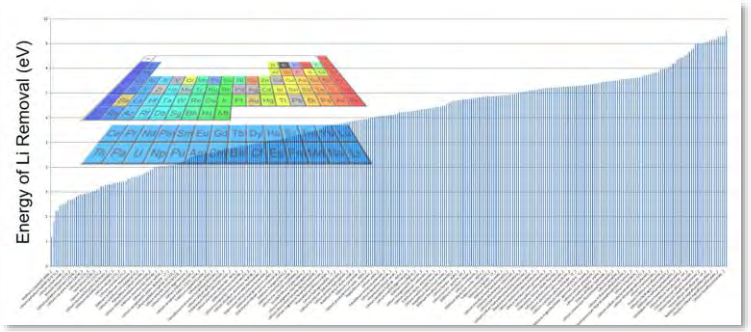

materials design

Hierarchy of Computational Approaches

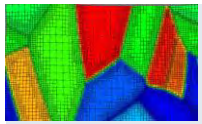

Continuum (finite element)

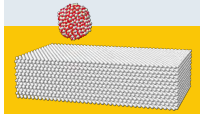

Interatomic potentials (forcefields)

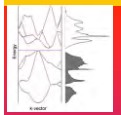

Ab initio quantum mechanics

- Hinges on the quality of input materials properties

- System specific
- Can be more accurate than ab initio, if calibrated with experimental data
- Computationally more efficient than ab initio; linear scaling

- General and free of system-specific parameters
- Standard DFT is extremely useful, but higher accuracy is highly desirable
- Computationally demanding, hence limited in model size and in configurational space

materials design

Examples

Plastic Deformation and Crack Propagation in Metals

$_{40}$Zr

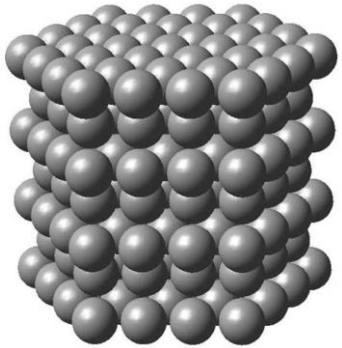

Machine learning for metallurgy V: A neural-network potential for zirconium

Manura Liyanage[1,*] David Reith[2] Volker Eyert[2] and W. A. Curtin[1]

[1]*Laboratory for Multiscale Mechanics Modelling, École Polytechnique Fédérale de Lausanne, CH-1015 Lausanne, Switzerland*

[2]*Materials Design SARL, 42 avenue Verdier, 92120 Montrouge, France*

Phys. Rev. Materials **6**, 063804 (2022)

Plastic Deformation

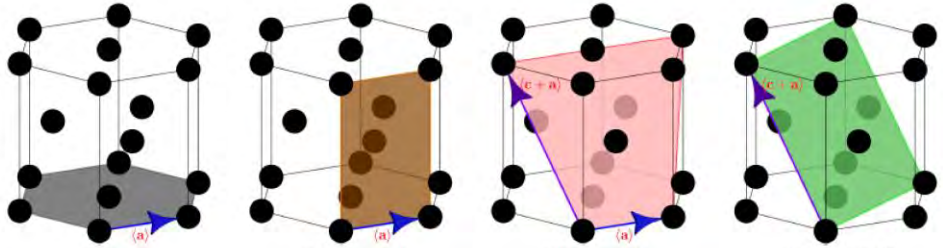

(a) Basal (b) Prismatic I (c) Pyramidal I (d) Pyramidal II

FIG. 1. Slip planes in the hcp crystal structure, where $\langle \mathbf{a} \rangle$ and $\langle \mathbf{c}+\mathbf{a} \rangle$ represent the $1/3\langle 1\bar{2}10 \rangle$ and $1/3\langle 1\bar{2}13 \rangle$ families of dislocations. Basal, prismatic I, pyramidal I, and pyramidal II are the $\{0001\}$, $\{10\bar{1}0\}$, $\{10\bar{1}1\}$, and $\{11\bar{2}1\}$ families of planes, respectively.

- The new neural network potential (NNP4) reproduces the DFT references far better than the Mendelev-Ackland #3 EAM potential.

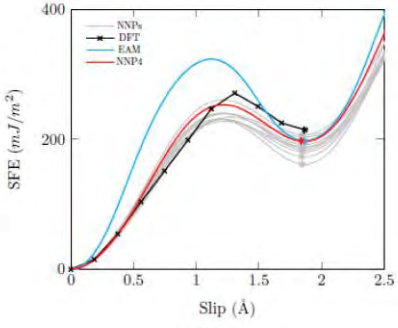

(a) Basal

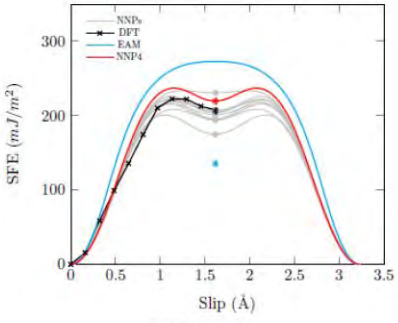

(b) Prismatic I-w

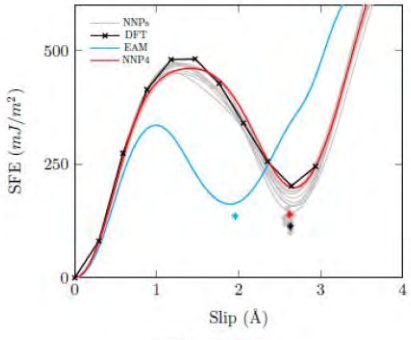

(c) Pyramidal I-w

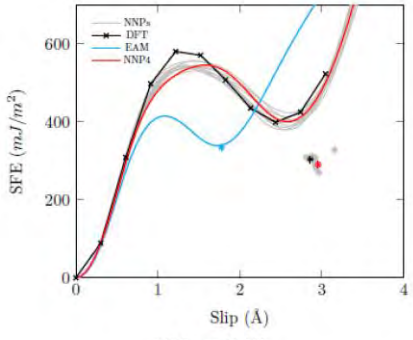

(d) Pyramidal II

materials design

Crack Formation in Zr Metal

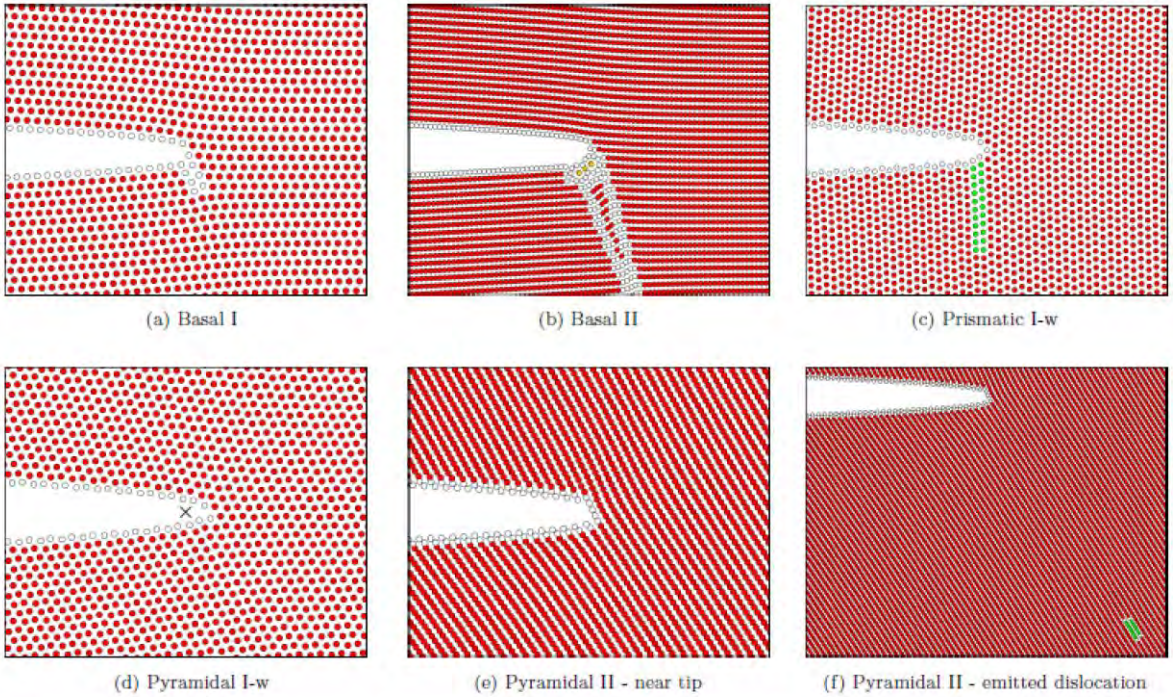

FIG. 14. Postfracture view of the near crack tip region for sharp crack tips obtained with the NNP4 potential, where red, green, and yellow circles represent atoms in hcp, fcc, and icosahedral crystal structures, respectively, and white circles represent atoms which cannot be classified to any structural system as identified by common neighbor analysis [86,87]. For the pyramidal I system, the initial crack tip location is shown with a "×". These structures are not contained in the training dataset.

The new neural network potential (NNP4) enables the investigation of the crack tip response, namely brittle cleavage and dislocation emission that blunts the crack tip, thereby encouraging ductility.

The two critical quantities are surface energies and unstable stacking fault energy. Both are accurately described by the current NNP, thus giving confidence to the current predictions.

Computational Approach

- Generation of a training set with VASP consisting of 1875 different structures containing a total of about 100,000 atoms in different local environments, *e.g.*, strained structures and trajectories from *ab initio* molecular dynamics
- Fitting to a neural network potential of the Behler-Parrinello form
- Model building, VASP computations, and the fitting were performed within the *MedeA* computational environment.

Structure of Grain Boundaries in Ceramics: m-ZrO_2

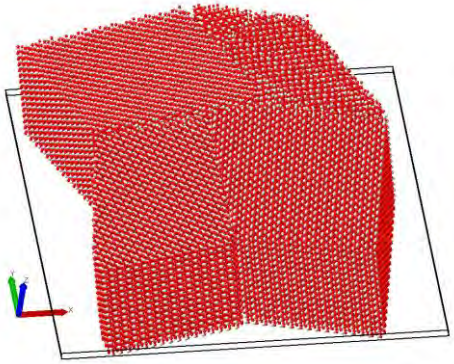

Initial model

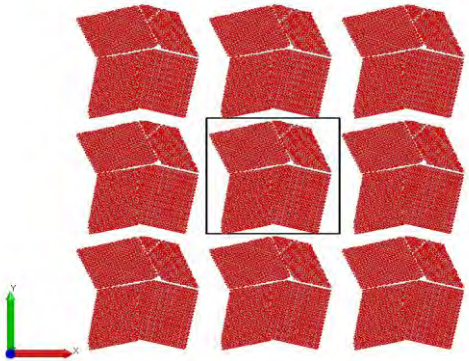

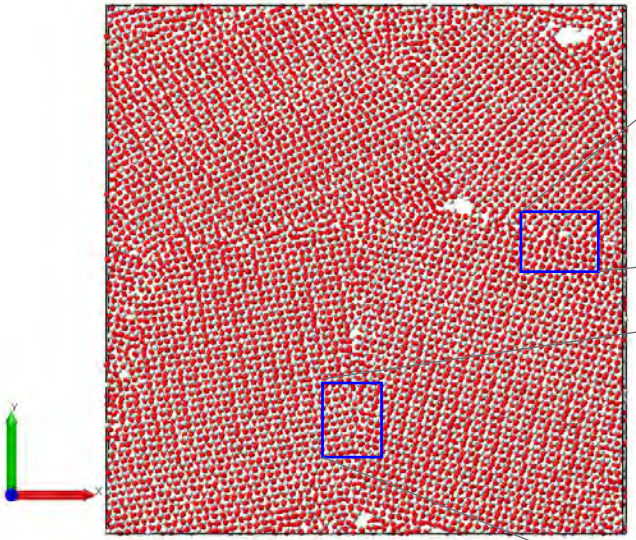

After annealing under 3 GPa at 600 K and further relaxation at 1 bar and 600 K

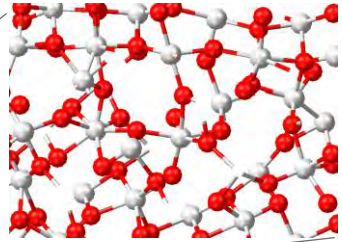

1 nm

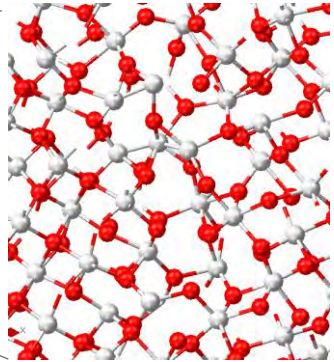

- The grain boundaries have a thickness of about 1 nm with local atomic coordination similar to that in the bulk.

materials design

m-ZrO_2 Grain Boundaries

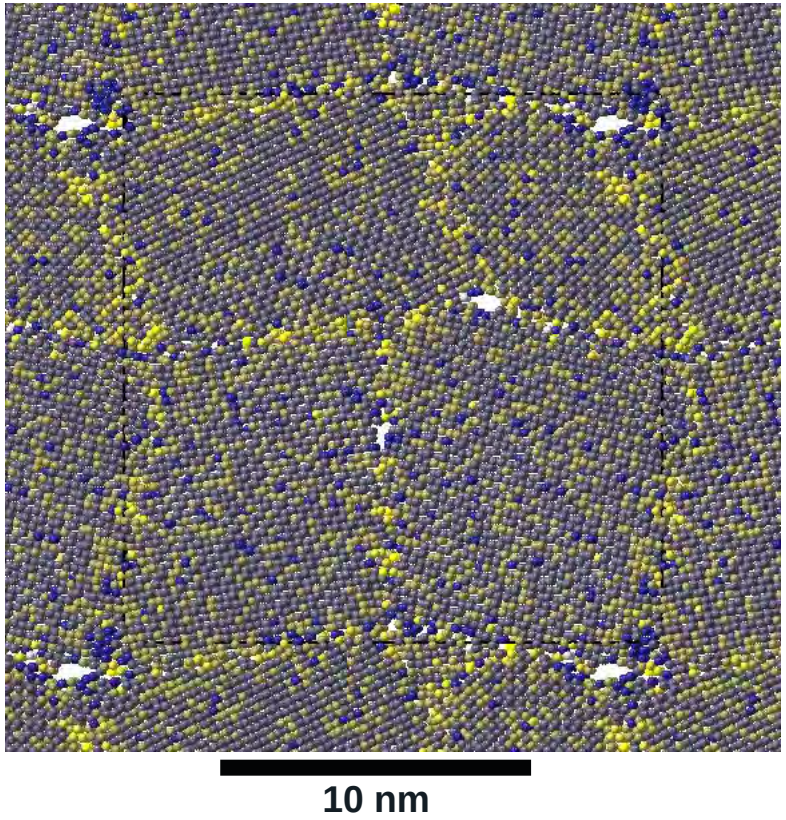

Energy of Zr atoms in grain boundary model of m-ZrO_2 shown in a cut perpendicular to the long axis of columnar crystallites.

Blue: energetically most stable Zr atoms
Yellow: energetically less favorable Zr atoms

Workflow:

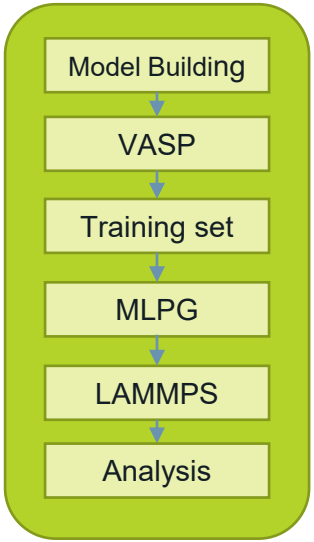

all in *MedeA*

materials design

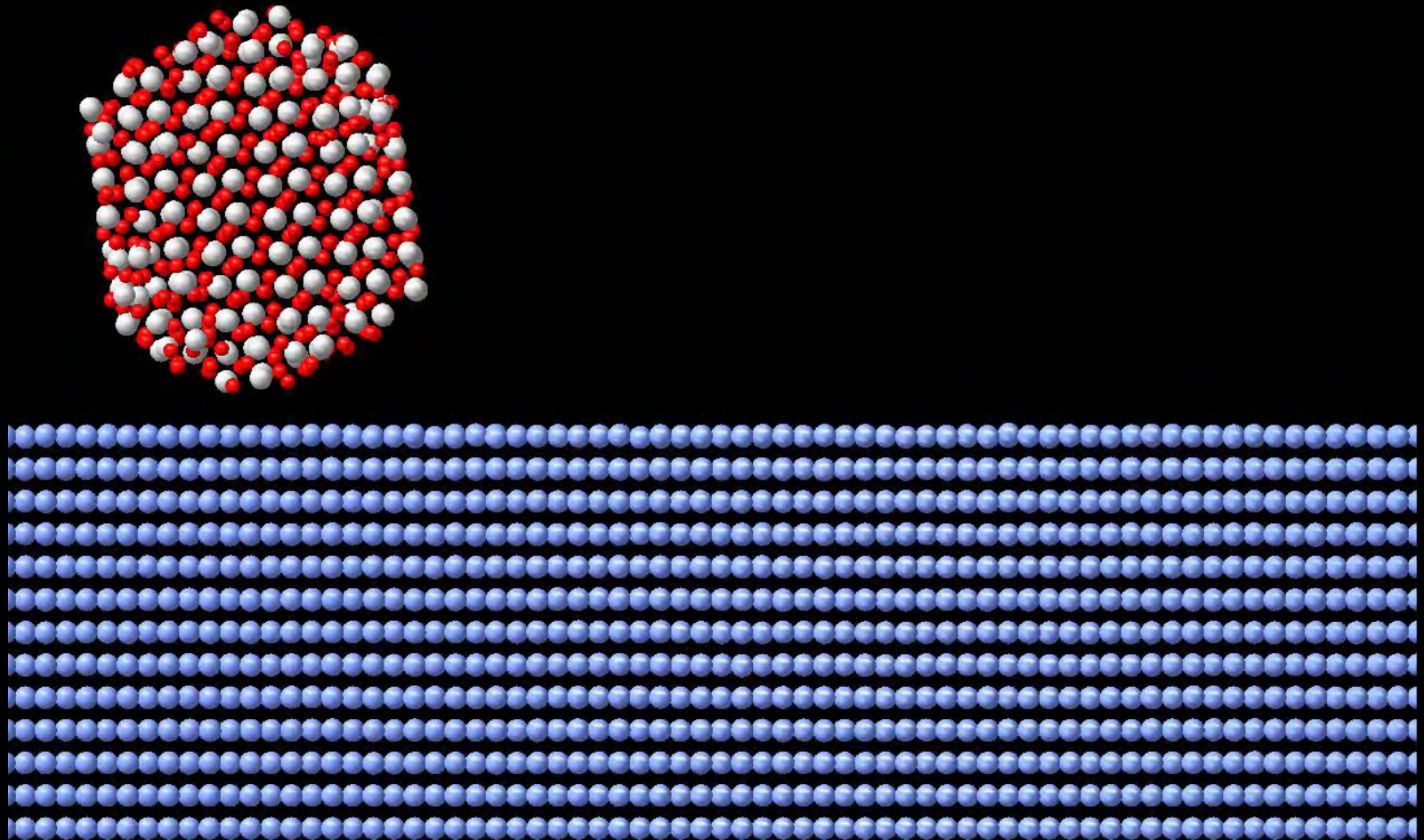

VASP

Total energies beyond DFT

One-electron/QP picture

DFT: Kohn-Sham eq.

$$\left(-\frac{1}{2}\Delta + V_{\mathrm{ext}}(\mathbf{r}) + V_{\mathrm{H}}(\mathbf{r}) + V_{\mathrm{xc}}\left[\rho\right](\mathbf{r})\right)\psi_{n\mathbf{k}}(\mathbf{r}) = \epsilon_{n\mathbf{k}}\psi_{n\mathbf{k}}(\mathbf{r})$$

Catalysis: dehydrogenation of propane in Mordenite

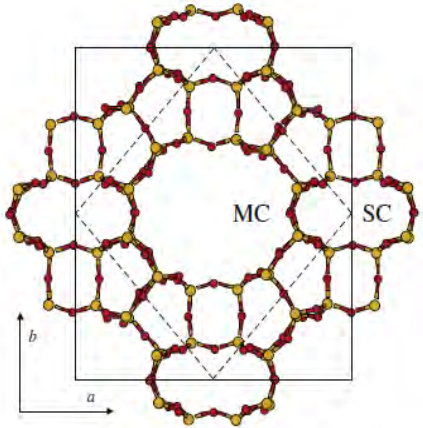

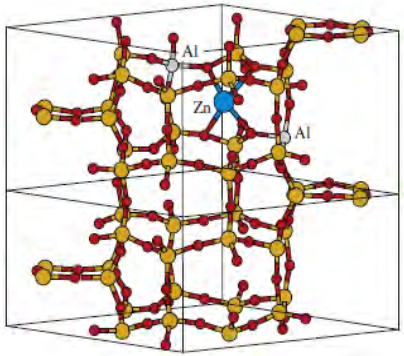

L. Benco et al./Journal of Catalysis 277 (2011) 104–116

$$\mathrm{MOR{-}Zn + C_3H_8 \rightarrow MOR{-}Zn\cdots C_3H_8},$$
$$\mathrm{MOR{-}Zn\cdots C_3H_8 \rightarrow H{-}MOR{-}Zn{-}C_3H_7},$$
$$\mathrm{H{-}MOR{-}Zn{-}C_3H_7 \rightarrow MOR{-}Zn\cdots C_3H_6 + H_2}$$
$$\mathrm{MOR{-}Zn\cdots C_3H_6 \rightarrow MOR{-}Zn + C_3H_6}.$$

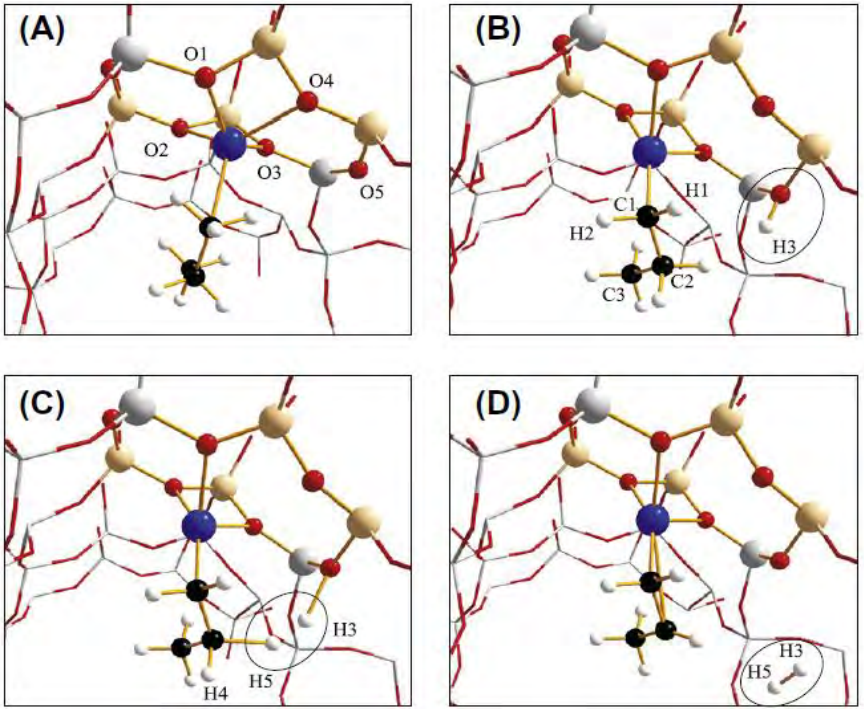

materials design

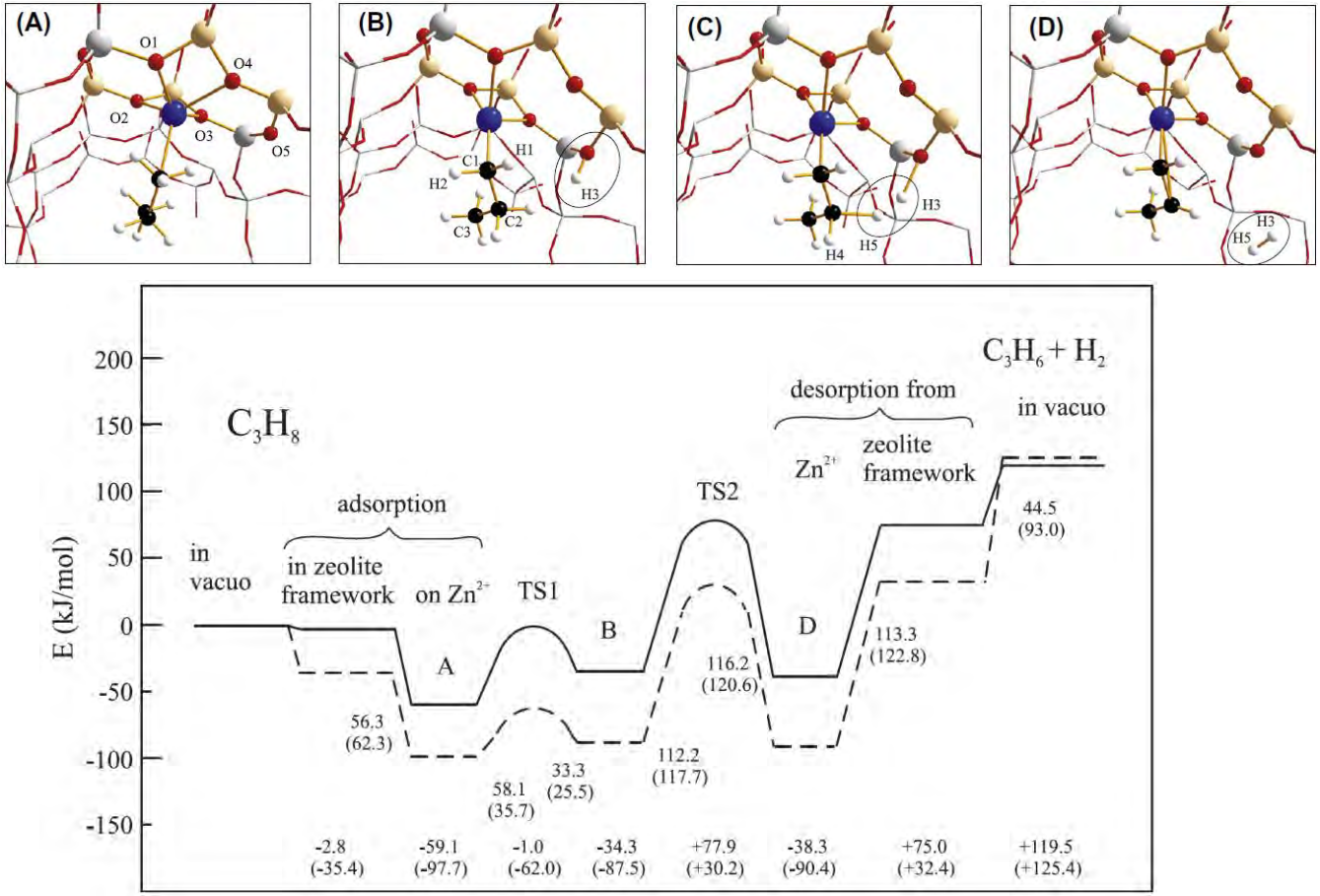

L. Benco *et al.*, Journal of Catalysis 227, 104 (2011)

CO adsorption on d-metal surfaces

- DFT incorrectly predicts that CO prefers the hollow site: P. Feibelman *et al.*, J. Phys. Chem. B 105, 4018 (2001)
- This error is relatively large. Best DFT/PBE calculations:

CO@Cu(111):	-170 meV
CO@Rh(111):	-40 meV
CO@Pt(111):	-100 meV

- CO HOMO-LUMO gap too small in DFT:

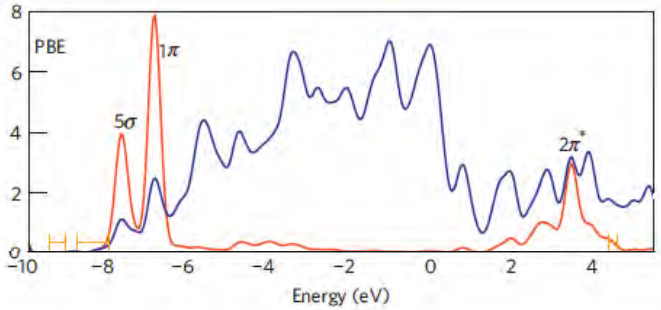

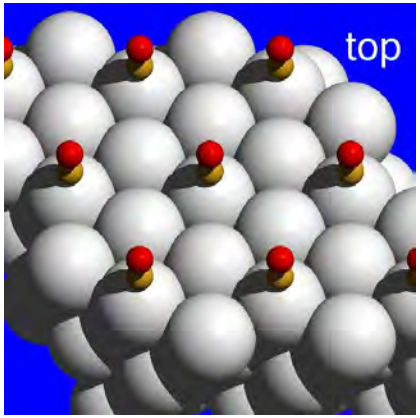

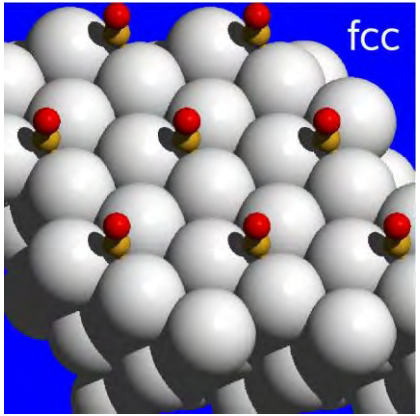

Need to go beyond DFT?

Lattice constants and Bulk moduli:
AlP, AlAs, BAs, BP, Si, C, SiC, MgO, LiF

	LDA		PBE		HF	
	Δa_0	ΔB_0	Δa_0	ΔB_0	Δa_0	ΔB_0
MRE	-1.4	3.5	0.8	-7.2	0.4	8.2
MARE	1.4	7.9	0.8	7.2	0.7	8.2

(All in %)

ΔH (kJ/mol)	PBE	EXP
$Al+N_2 \rightarrow AlN$	262	350
$Mg+H_2 \rightarrow MgH_2$	52	78
$Si+C \rightarrow SiC$	51	69
$CO \rightarrow CO@Rh$	183	144

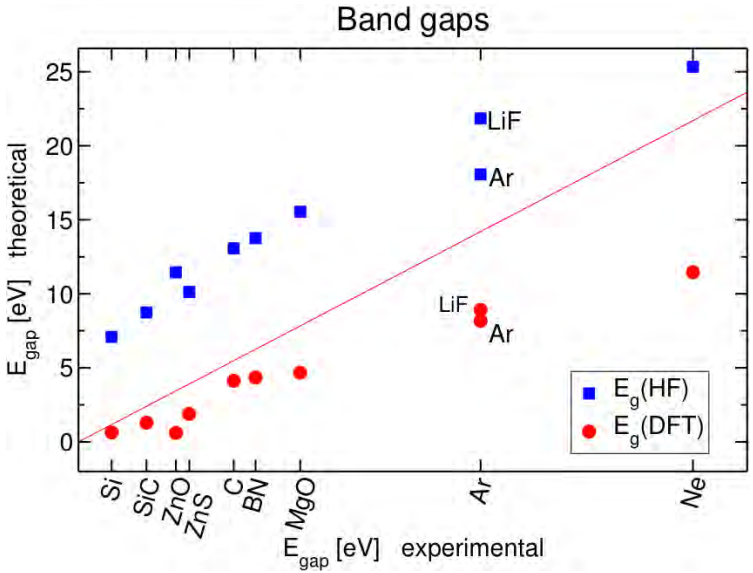

(More) accurate treatment of electronic correlation needed for, e.g:

- Band gaps (optical properties)
- Total energy differences with "chemical accuracy" (1 kcal/mol ≈ 40 meV): Atomization-, formation energies, reaction barriers, *etc*
- Van der Waals interactions

materials design

One-electron/QP picture

DFT: Kohn-Sham eq.

$$\left(-\frac{1}{2}\Delta + V_{\text{ext}}(\mathbf{r}) + V_{\text{H}}(\mathbf{r}) + V_{\text{xc}}\left[\rho\right](\mathbf{r})\right)\psi_{n\mathbf{k}}(\mathbf{r}) = \epsilon_{n\mathbf{k}}\psi_{n\mathbf{k}}(\mathbf{r})$$

DFT-HF hybrid functionals: Roothaan eq.

$$\left(-\frac{1}{2}\Delta + V_{\text{ext}}(\mathbf{r}) + V_{\text{H}}(\mathbf{r})\right)\psi_{n\mathbf{k}}(\mathbf{r}) + \int V_{\text{X}}\left[\{\psi_o\}\right](\mathbf{r},\mathbf{r}')\psi_{n\mathbf{k}}(\mathbf{r}')d\mathbf{r}' = \epsilon_{n\mathbf{k}}\psi_{n\mathbf{k}}(\mathbf{r})$$

Hybrid functionals

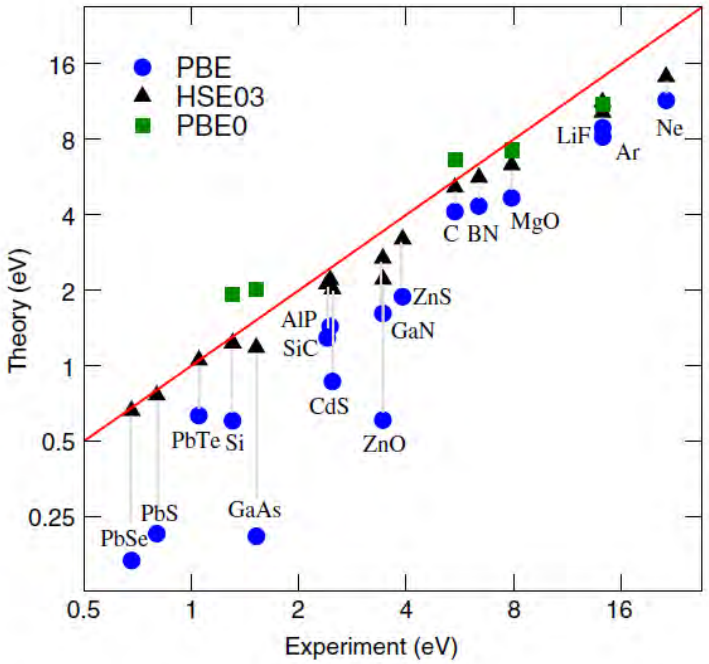

Figure 8. Band gaps from PBE, PBE0, and HSE03 calculations, plotted against data from experiment.

Lattice constant

	MRE	MARE
PBE	0.8	1.0
PBE0	0.1	0.5
HSE	0.2	0.5
B3LYP	1.0	1.2

Bulk modulus

	MRE	MARE
PBE	-9.8	9.4
PBE0	-1.2	5.7
HSE	-3.1	6.4
B3LYP	-10.2	11.4

Atomization energy

	MRE	MARE
PBE	-1.9	3.4
PBE0	-6.5	7.4
HSE	-5.1	6.3
B3LYP	-17.6	17.6

(All in %)

materials design

CO adsorption on d-metal surfaces

CO @		top	fcc	hcp	Δ
Cu(111)	PBE	0.709	0.874	0.862	−0.165
	PBE0	0.606	0.579	0.565	0.027
	HSE03	0.561	0.555	0.535	0.006
	exp.	0.46-0.52			
Rh(111)	PBE	1.870	1.906	1.969	−0.099
	PBE0	2.109	2.024	2.104	0.005
	HSE03	2.012	1.913	1.996	0.016
	exp.	1.43-1.65			
Pt(111)	PBE	1.659	1.816	1.750	−0.157
	PBE0	1.941	1.997	1.944	−0.056
	HSE03	1.793	1.862	1.808	−0.069
	exp.	1.43-1.71			

(All energies in eV)

A. Stroppa *et al.*, PRB 76, 195440 (2007); A. Stroppa and G. Kresse, NJP 10, 063020 (2008).

Hybrid functionals reduce the tendency to stabilize adsorption at the hollow site w.r.t. the top site.

reduced CO $2\pi^*$ – metal-*d* interaction

- DFT does well for the metallic surface, but not for the CO: $2\pi^*$ (LUMO) too close to the Fermi level.
- HSE does well for the CO, but not for the surface: *d*-metal bandwidth too large.

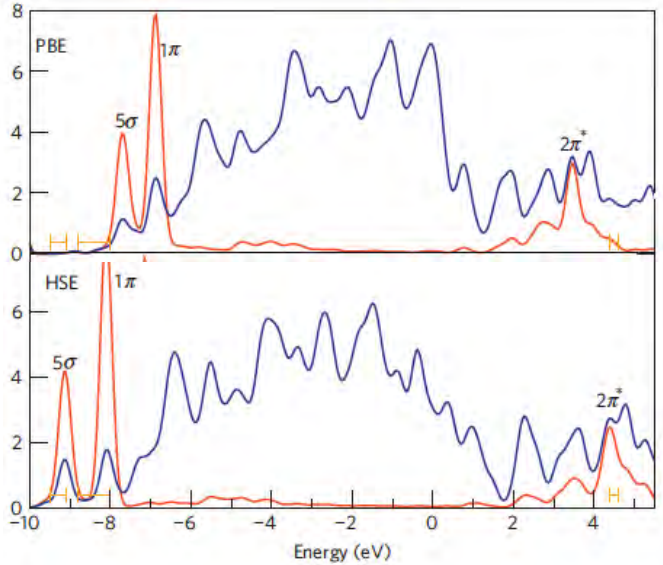

Schimka et al., Nature Materials 9, 741 (2010)

materials design

Need to go beyond DFT and DFT/HF hybrids?

Heats of formation

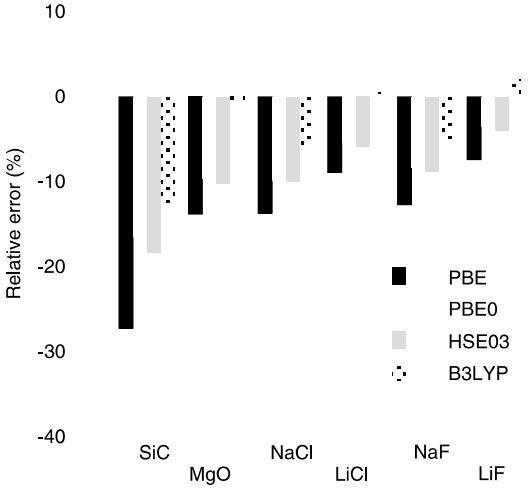

- Total energy differences with "chemical accuracy" (1 kcal/mol ≈ 40 meV/atom): Atomization-, formation energies, reaction barriers, *etc*
- Van der Waals interactions

Bandgaps

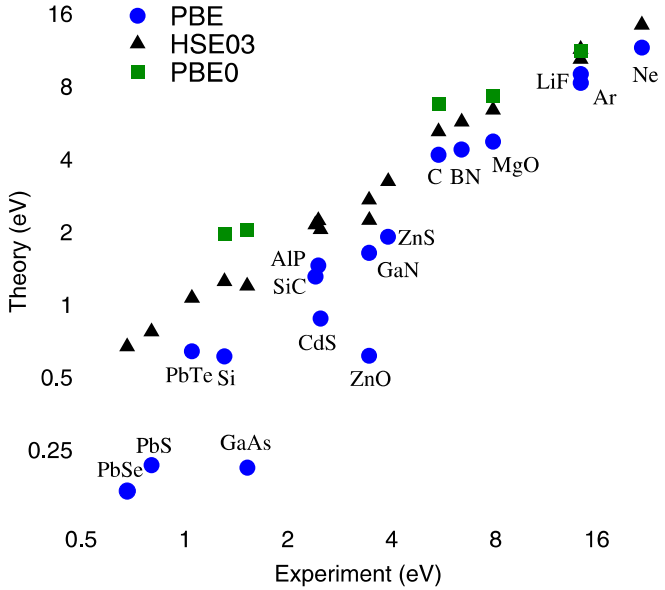

- Bandstructure of metals and *largish* gap systems, and some problematic cases in between

materials design

One-electron/QP picture

DFT: Kohn-Sham eq.

$$\left(-\frac{1}{2}\Delta + V_{\text{ext}}(\mathbf{r}) + V_{\text{H}}(\mathbf{r}) + V_{\text{xc}}\left[\rho\right](\mathbf{r})\right)\psi_{n\mathbf{k}}(\mathbf{r}) = \epsilon_{n\mathbf{k}}\psi_{n\mathbf{k}}(\mathbf{r})$$

DFT-HF hybrid functionals: Roothaan eq.

$$\left(-\frac{1}{2}\Delta + V_{\text{ext}}(\mathbf{r}) + V_{\text{H}}(\mathbf{r})\right)\psi_{n\mathbf{k}}(\mathbf{r}) + \int V_{\text{X}}\left[\{\psi_o\}\right](\mathbf{r},\mathbf{r}')\psi_{n\mathbf{k}}(\mathbf{r}')d\mathbf{r}' = \epsilon_{n\mathbf{k}}\psi_{n\mathbf{k}}(\mathbf{r})$$

GW: quasi-particle eq.

$$\left(-\frac{1}{2}\Delta + V_{\text{ext}}(\mathbf{r}) + V_{\text{H}}(\mathbf{r})\right)\psi_{n\mathbf{k}}(\mathbf{r}) + \int \Sigma\left[\{\psi, E\}\right](\mathbf{r},\mathbf{r}', E_{n\mathbf{k}})\psi_{n\mathbf{k}}(\mathbf{r}')d\mathbf{r}' = E_{n\mathbf{k}}\psi_{n\mathbf{k}}(\mathbf{r})$$

Graphite vs. Diamond

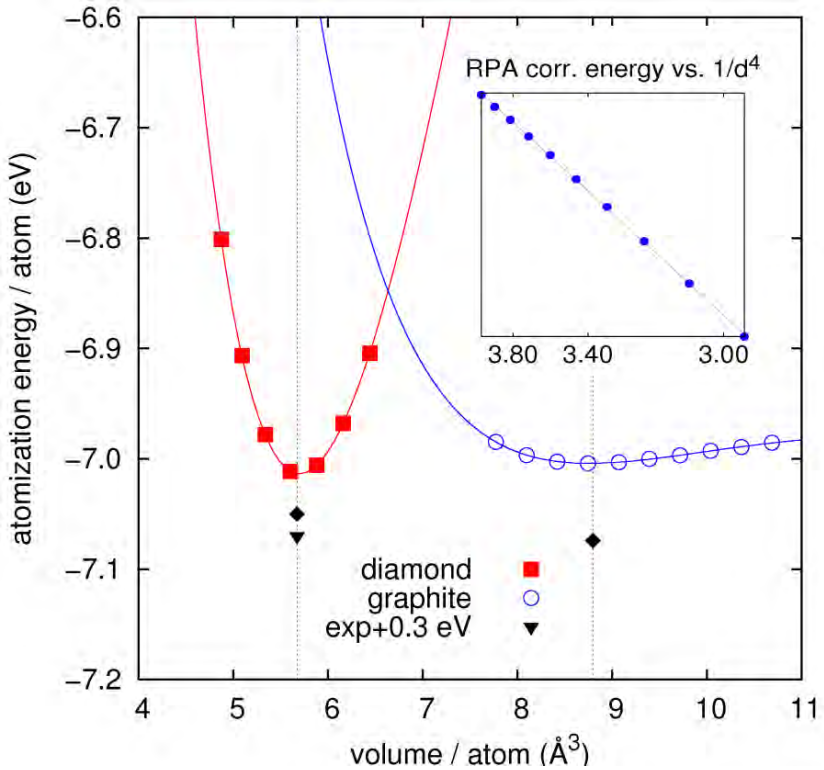

$1/d^4$ behavior at short distances

	QMC (Galli)	RPA	EXP
d(Å)	3.426	3.34	3.34
C_{33}		36	36-40
E(meV)	56	48	43-50

J. Harl, G. Kresse,
PRL 103, 056401 (2009).
S. Lebeque, et al.,
PRL 105, 196401 (2010).

materials design

RPA: CO @ Pt(111) and Rh(111)

Schimka et al., Nature Materials 9, 741 (2010)

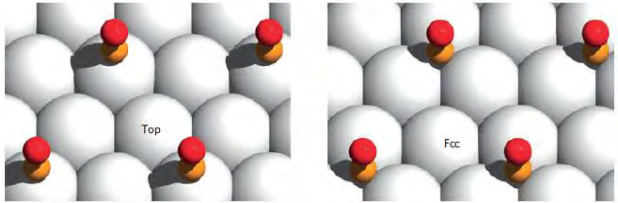

RPA:

- increases surface energy and
- decreases adsorption energy

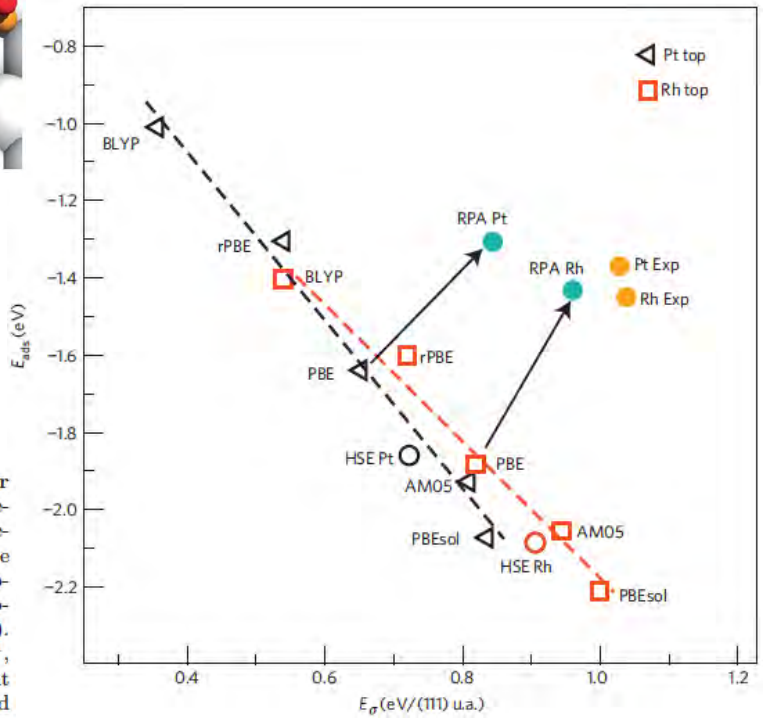

FIG. 1: **Atop CO adsorption and surface energies for Pt(111) and Rh(111).** (a) Considered CO adsorption geometries for a (2×2) surface cell. Semi-local functionals predict CO to adsorb in the fcc hollow site coordinated to three metal atoms on Pt and Rh, whereas experiments unequivocally show adsorption atop a metal atom. (b) Atop adsorption energies versus surface energies for Pt(111) and Rh(111). Various semi-local functionals were used: AM05[10], PBEsol[11], PBE[8], rPBE[12] and BLYP[13], in order of increasing gradient corrections. Furthermore the hybrid functional HSE[18] based on the PBE functional was used.

materials design

- DFT does well for the metallic surface, but not for the CO: $2\pi^*$ (LUMO) too close to the Fermi level.

- HSE does well for the CO, but not for the surface: *d*-metal bandwith too large.

- GW gives a good description of both the metallic surface as well as of the CO $2\pi^*$ (LUMO). The CO 5σ and 1π are slightly underbound.

Schimka et al., Nature Materials 9, 741 (2010)

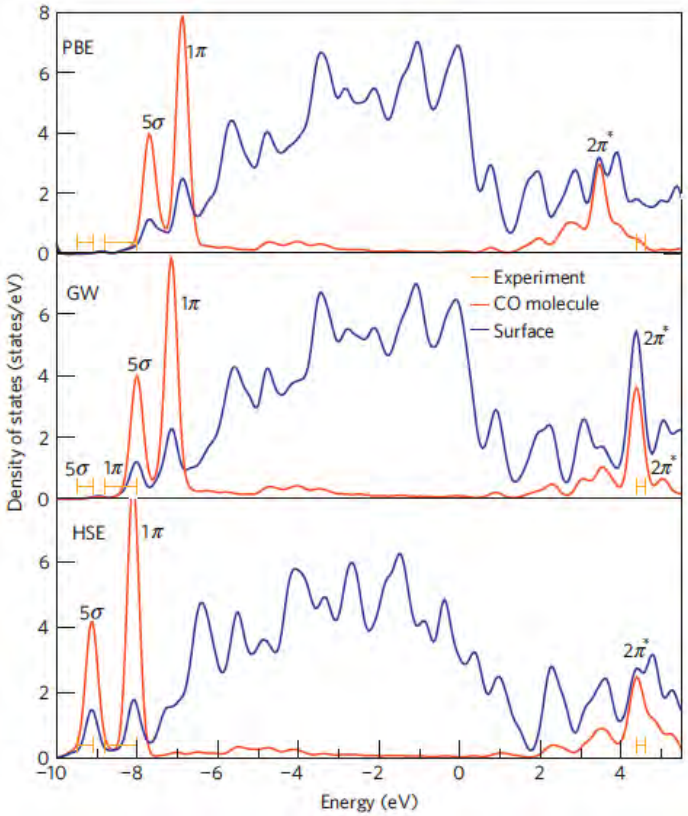

Figure 2 | Electronic DOS for CO adsorbed atop a Pt atom on Pt(111). The DOS is evaluated using DFT (PBE), the RPA (GW) and a hybrid functional (HSE). Experimental photoemission data for the $2\pi^*$ state are from ref. 19, for the 5σ and 1π state from ref. 20.

materials design

RPA:

- Right site preference
- Good adsorption energies
- Excellent lattice constants
- Good surface energies

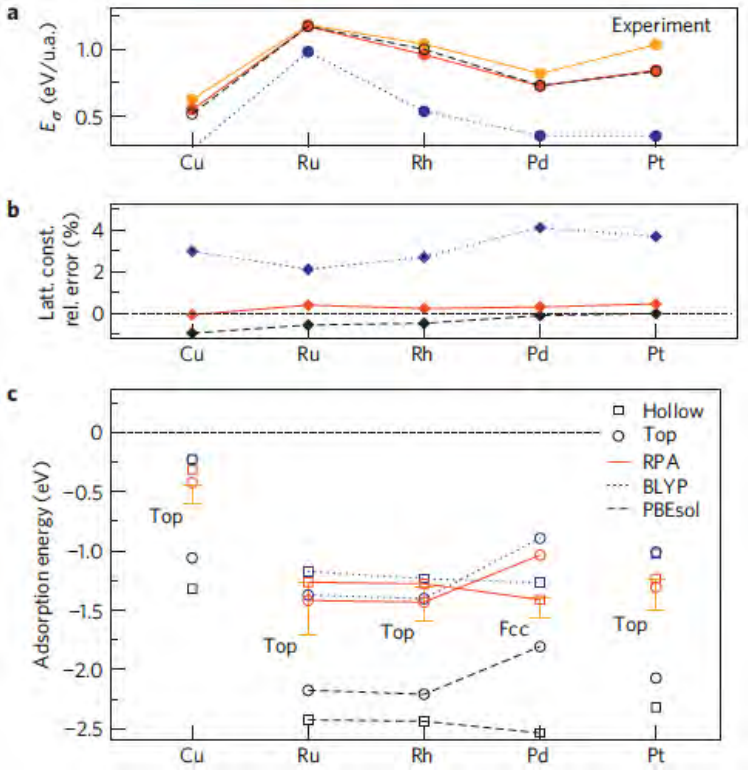

Figure 3 | Surface energies, lattice constants and adsorption energies. **a**, Fcc(111) surface energies (E_σ) for PBEsol, BLYP and RPA. Experimental surface energies are deduced from liquid-metal data[24,25]. **b**, Lattice constants for PBEsol, RPA and BLYP. **c**, Adsorption energies for the atop and hollow sites of CO on Cu, late 4*d* metals and Pt for PBEsol, RPA and BLYP. Experimental data with error bars are from ref. 26. The error bars correspond to the spread of the experimental results.

Schimka et al., Nature Materials 9, 741 (2010)

RPA: heats of formation

Heats of formation w.r.t. normal state at ambient conditions (in kJ/mol)

Example: Mg(bulk metal) + $H_2 \rightarrow MgH_2$

	PBE	Hartree-Fock	RPA	EXP
LiF	570	664	609	621
NaF	522	607	567	576
NaCl	355	433	405	413
MgO	516	587	577	603
MgH_2	52	113	72	78
AlN	262	350	291	321
SiC	51	69	64	69

J. Harl and G. Kresse, PRL 103, 056401 (2009)

materials design

State of the Art

- Beyond DFT: the RPA
  - Well balanced description of all bond types (metallic, covalent, ionic, vdW)
  - Cubic-Scaling
  - Finite temperature
  - Forces and stress
  - At present, RPA offers an optimal balance between accuracy and computational effort
  - More fundamental work is needed to reach chemical accuracy

Δ – learning

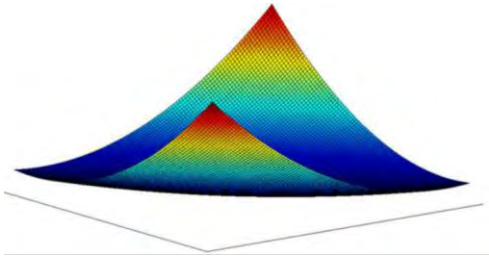

Dataset $T^{(2)}$ (1275 structures of 24 atoms, $QM_{(L)}$)

2nd on-the-fly active learning

SVD rank compression

Dataset $T^{(3)}$ (168 structures of 24 atoms, $QM_{(L)}$ and $QM_{(H)}$)

$\Delta=QM_{(H)}-QM_{(L)}$

MLFF-Δ

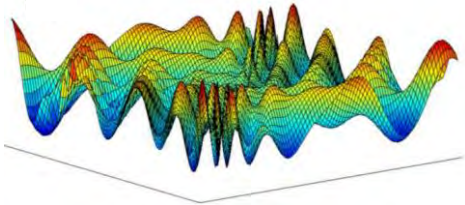

1st on-the-fly active learning

Dataset $T^{(1)}$ (592 structures of 96 atoms, $QM_{(L)}$)

$MLFF\text{-}QM_{(L)}$

Corrected dataset $T^{(1')}$ (592 structures of 96 atoms, $QM_{(L)}+\Delta$)

$MLFF\text{-}QM^{\Delta}_{(H)}$

MLFF-Δ(RPA): P. Liu, C. Verdi, F. Karsai, and G. Kresse, PRB 105, L060102 (2022)

Temperature-induced Phase Transitions of Zirconia

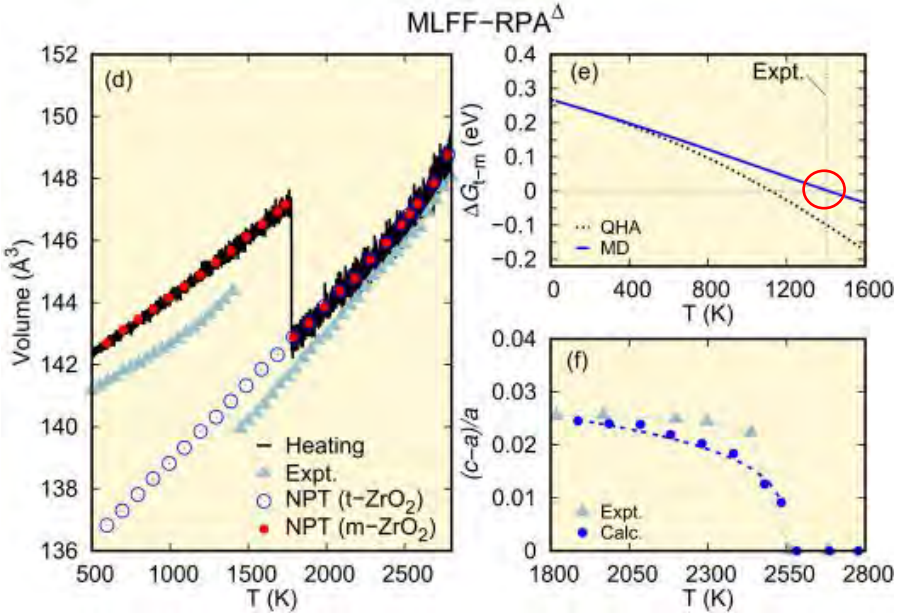

	PBE	SCAN	MLFF-SCAN	MLFF-RPA$^{\Delta}$	Expt.
Monoclinic					
Volume	36.15	35.35	35.37	35.20	35.22
Tetragonal					
Volume	34.70	33.82	33.90	33.47	33.01
ΔE_{t-m}	0.110	0.074	0.074	0.067 (0.069)	
ΔH_{t-m}			0.069	0.069	0.056(3)
$T_c(t-m)$			1492	1415	1400
Cubic					
Volume	33.56	32.92	32.97	32.70	
ΔE_{c-t}	0.102	0.085	0.083	0.053 (0.047)	
$T_c(c-t)$			2585	2546	2570

P. Liu, C. Verdi, F. Karsai, and G. Kresse, Phys. Rev. B **105**, L060102 (2022).

Summary

- Electronic structure calculations with VASP provide a state-of-the-art foundation for multi-scale simulations
- The efficient generation of high-quality machine-learned potentials enables atomistic simulations at unprecedented levels of accuracy as demonstrated in this webinar:
  - Plastic deformation and crack propagation in metals
  - Grain boundaries in ceramics
  - Impact of nanoparticles on surfaces
- Workflows as implemented in *MedeA* in the form of flowcharts and the concept of *MedeA* structure lists make complex modeling protocols readily practical, such as the creation of MLP training sets with VASP, the generation of MLP's, and their use in molecular dynamics simulations with LAMMPS.
- High accuracy on RPA level for large systems enabled with delta-learning
  - Temperature induced phase transitions in zirconia

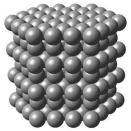

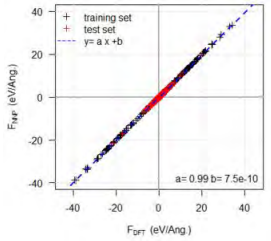

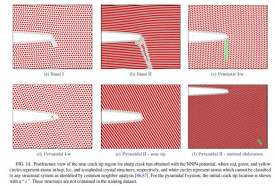

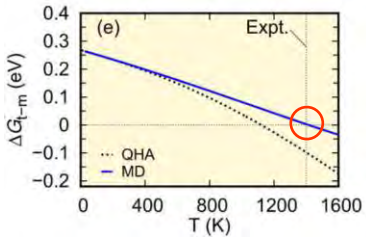

materials design

Acknowledgements

All customers of Materials Design

All science and technology partners, especially

Georg Kresse and the entire VASP team

All colleagues at Materials Design, especially

Benoit Leblanc	Leonid Kahle
Benoit Minisini	Marianna Yiannourakou
Clint Geller	Mikael Christensen
Clive Freeman	Ray Shan
Dave Rigby	René Windiks
David Reith	Volker Eyert
Jörg-Rüdiger Hill	Walter Wolf
Kyle Starkey	Xavier Rozanska

Question and Answer Session

Erich Wimmer

Materials Design

Martijn Marsman

University of Vienna

Highlighted Modules

VASP accuracy with LAMMPS speed at your fingertips all within *MedeA*

- *MedeA VASP* offers a comprehensive graphical user interface (GUI) to set up, run and analyze multi-step VASP calculations. *MedeA* provides tools for automation of more complex computational tasks such as automated convergence tests and a flowchart type environment to automate work flows, combine computational techniques, and enable high-throughput screening. Full integration in the *MedeA Environment* with a GUI and proven default values, combined with support and training turn VASP into *MedeA VASP*: Fast learning and progress in pace with current industrial demands.
- Machine Learned Potentials (MLPs) offer a combination of extended length and time scales with unprecedented ease in generation and high fidelity with respect to DFT to describe so far inaccessible physical phenomena.
- The *MedeA* MLP Generator (MLPG) offers a fully integrated workflow from training-set generation (using *MedeA* HT) and MLP generation to MLP application using *MedeA* LAMMPS.
- MedeA HT With the modules *MedeA HT-Launchpad* and *MedeA HT-Descriptors*, *MedeA* offers unique, powerful, yet very easy to use tools to accomplish these modeling tasks. *MedeA's* HT modules enable you to generate large and consistent sets of computed data and to create descriptors combining experimental and computed properties to screen, understand, and optimize materials, thus creating the input for machine learning procedures.

Question and Answer Session

Erich Wimmer

Materials Design

Martijn Marsman

University of Vienna

Questions about Materials Design Webinars

Katherine Hollingsworth

khollingsworth@materialsdesign.com

materials design

info@materialsdesign.com

www.materialsdesign.com

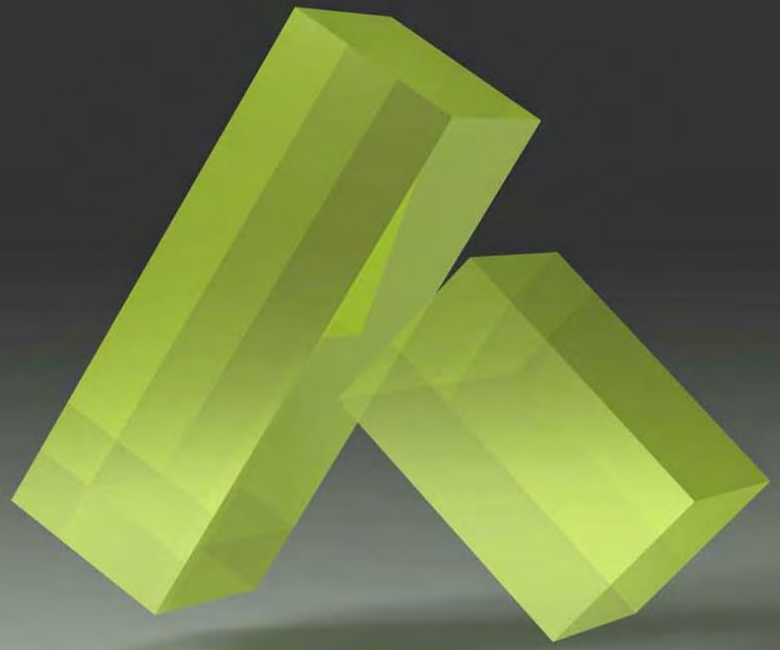

MedeA

Innovation by Simulation